Novel application of large area propeller to optimize Energy Efficiency Design Index (EEDI) of ships

P Duplex (Alumni of Erasmus Mundus Masters program in Naval Architecture: Emship), The Netherlands.
T Bugalski, M Kraskowski, **P Hoffmann** (Ship Hydromechanics Division, Ship Design and Research Centre, Gdańsk, Poland).
Z Sekulski, (West Pomeranian University of Technology, Szczecin, Poland).

SUMMARY

After globalization environmental pollution and rising fuel costs are posing a major threat to the shipping industry. The reduction of CO_2 emissions has been the key target since IMO's Marine Environment Protection Committee (MEPC) published its findings in 2009. A number of measures resulting in technical and operational reductions were made mandatory in 2011. Among these and nearly all new build ships [9] have to conform is Energy Efficiency Design Index (EEDI). This provides a method of establishing the minimum efficiency of new ships depending on the type and size. With increasing competition the key to survival will be to design and operate the ships efficiently. In the current phase designers relied to retrofit methods and achieved slight gains of hull efficiency. In later phases tougher restrictions will be imposed which needs more changes in ship design. This work is based on propeller relocation as demonstrated in the R&D project "Streamline" initiated by the seventh frame work of European commission which resulted in significant savings in delivered power. An extensive analysis is made in the CFD code Star-CCM+ at Centrum Techniki Okrętowej S.A., Gdańsk, Poland (CTO) during an internship.

1 INTRODUCTION

Melting glaciers, rising sea levels, depleting forests and reducing wildlife are the evident of climate change. These climate changes are mainly due to the human activities such as deforestation and burning fossil fuels which increase the concentration of green house gases [3]. Excessive CO_2 in the air makes the green house effect stronger and in turn rises the average temperature of earth's atmosphere and oceans causing global warming and related consequences.

1.1 SHIPPING INDUSTRY

Shipping industry is one of the biggest contributor of the green house gases and thus plays a part in global warming. As seen in figure 1 its contribution is comparable to the CO_2 emission from a country like Germany. According to IMO's second greenhouse gas study [2] shipping is measured to have emitted 1046 million tons of CO_2 during 2007.Even though CO_2 emissions from ships accounts for 3% of the global emissions it is by far most efficient mode of commercial transport as a cargo vessel of <8000DWT emits only 15 grams of CO_2 per tonne-km comparing 50g/t-km of heavy truck and 540 g/t-km of airfreight. Figure 4 gives an overview of CO_2 emissions from various types of ships between 2007-2012.

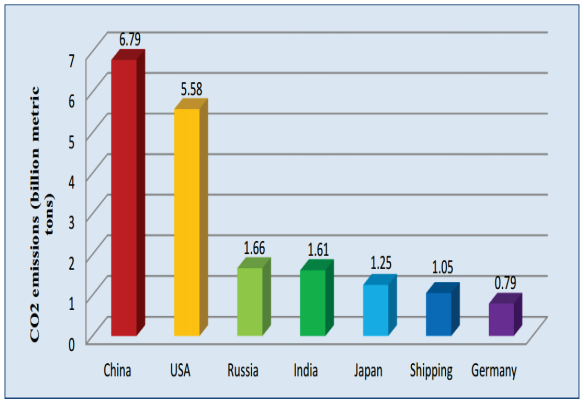

Figure 1: Shipping VS CO_2 emission from major economies. [2]

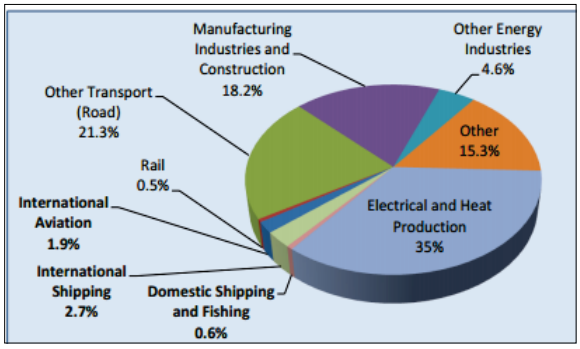

Figure 2: Sector wise CO_2 emission comparison [2]

1.2 PROJECTED GROWTH OF CO_2 EMISSIONS

Marine transport's global carbon foot print is projected to grow, due to the heavy reliance of ships on oil for propulsion, and the expected growth in the world trade driven by expanding global population, world economy and demand for shipping services. According to IMO findings, in the absence of policies as a result of the growth in shipping, CO_2 emissions from international shipping may grow by a factor of 3 as compared to the emissions of 2007, which is projected as 12-18% of global total emissions in 2050 [5]. It also states that without any policies being enforced this will lie between 6-22% (925-1058Mt of CO_2 emissions) higher in 2020 than that of 2007.

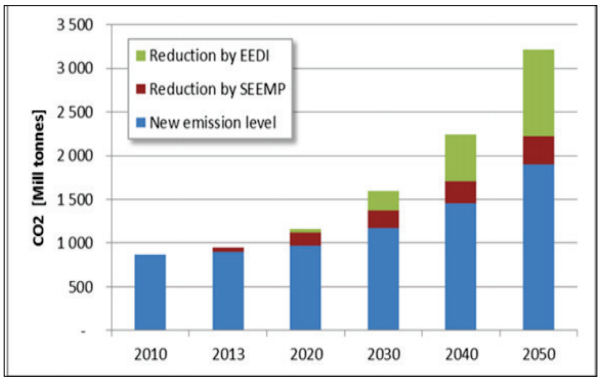

Figure 3: Projected emission control due to regulations [1]

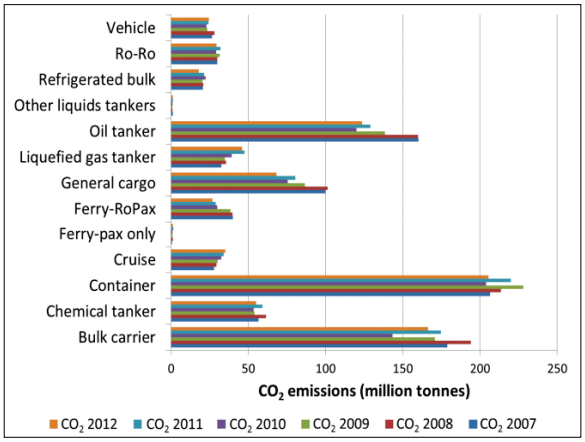

Figure 4: CO2 emissions 2007-2012 [1]

2 DEVELOPMENT OF EMISSION INDEX IN IMO

On the 62nd MEPC session new regulation was adopted which was the first global CO_2 emission control index in the industry [16]. The amendments to MARPOL Annex VI regulations for the prevention of air pollution from ships add a new chapter 4 to Annex VI on regulations on energy efficiency for ships to make mandatory the Energy Efficiency Design Index (EEDI) for new ships and the Ship Energy Efficiency Management Plan(SEEMP) for all ships. The application of the EEOI remains non mandatory but it has been included in the ship Energy Efficiency Management Plan (SEEMP) as a possible index to verify and measure its effectiveness. While IMO decided not to use the EEOI indicator as a basis for regulation.

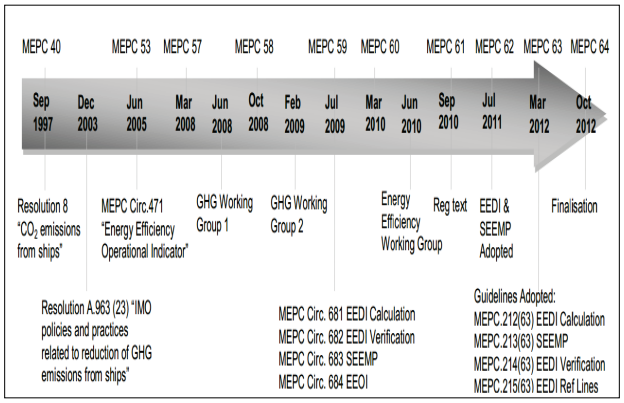

Figure 5: IMO's timeline [15]

2.1 ENERGY EFFICIENCY DESIGN INDEX (EEDI)

The energy efficiency design index (EEDI) was formally adopted by the IMO in July 2011 and applies to new ships built from 2013 onwards. It can be considered as a performance based tool that allows ship designers and builders to choose from various available cost effective technologies that can be used for a specific ship design. The EEDI provides a specific figure for an individual ship design expressed in grams of CO_2 per ship's capacity mile (smaller value indicates better efficiency).The

formulation takes in to account ship's emissions, capacity and speed. There is a reference value and the attained EEDI value should be less than this.

2.1.1 Base Line Formulation

EEDI formula calculates the CO2 emission efficiency of a vessel at the design stage in terms of (g.CO_2/tonne-nm). IMO first developed the EEDI baseline from the data collected from existing ships using Lloyds fair play (LRFP) database. These baselines are developed for each category of ship like bulk carrier, container etc. The EEDI reference line refer to the statistically averaged EEDI curves derived from data from existing ships.

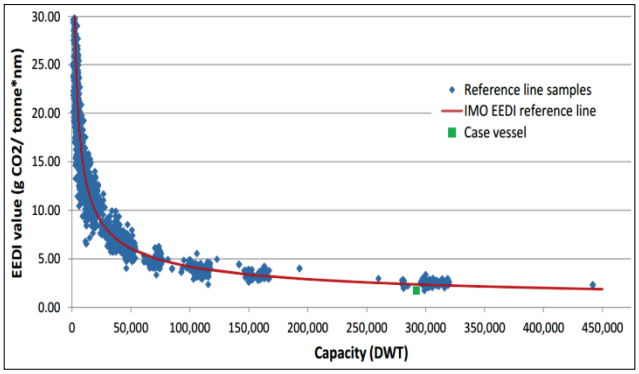

Figure 6: Baseline establishment [15]

Fuel consumption of an engine can be calculated as a product of produced power *(P)* and Specific fuel consumption *(SFC)*. So again,

$$EEDI=\frac{(P_{ME}\times SFC_{ME}\times C_{FME})+(P_{AE}\times SFC_{AE}\times C_{FAE})}{Capacity\times V_{ref}} \quad (4)$$

Power take in electrical motors (P_{PTI}) on propeller shaft are installed in some ships and the impact of these devices are also included.

Some ships are fitted with innovative energy saving technologies like sails, solar panels etc which reduce the power required either from main and auxiliary engines (P_{eff} *and* P_{AEeff}). These factors are taken care in the formula by subtracting the emission reduction due to innovative technologies.

2.1.2 The Formula

The basis of creating the index is to represent CO_2 efficiency of ship at design point.

$$EEDI=\frac{CO_2\ Emission}{Transport\ work} \quad (1)$$

The source of CO_2 emissions from ships comprises of emission from the main (CO_{2ME}) and auxiliary engines (CO_{2AE}) at certain power defined by the ship's operating speed. Transport work is the product of ship capacity (DWT) and speed (V_{ref}). It can written as,

$$EEDI=\frac{CO_{2ME}+CO_{2AE}}{Capacity\times V_{ref}} \quad (2)$$

The main and auxiliary engine emissions can be calculated by multiplying fuel consumption of the main and auxiliary engines with the carbon conversion factor (C_{FME} *and* C_{FAE} respectively) (C_f), which connects the fuel consumption to the amount of CO_2 emissions. Thus the formula becomes,

$$EEDI=\frac{(FC_{ME}\times C_{FME})+(FC_{AE}\times C_{FAE})}{Capacity\times V_{ref}} \quad (3)$$

Some ships with special design elements may require additional installed main power (ice class ships). This is taken care of by introducing a power correction factor (f_j) which normalizes the installed main engine power.

A capacity correction factor (f_i) is included in the formula because capacity of the ship may be limited due to technical or regulatory reasons. A weather correction coefficient (f_w) is included to normalise the speed of the ship as ships are designed for various operation conditions of wave height, wave frequency and wind speed. A cubic correction factor (f_c) is included to normalise the capacity for chemical tankers and gas carriers.

When these non dimensional factors are included and if multiple engines are taken into consideration the equation in full form can be shown as in equation 5,

$$\frac{\left[\left(\prod_{j=1}^{M} f_j\right)*\left(\sum_{i=1}^{nME} P_{ME(i)}*C_{FME(i)}*SFC_{ME(i)}\right)+\left(P_{AE}*C_{FAE}*SFC_{AE}\right)+\left(\left(\prod_{j=1}^{M} f_j*\sum_{i=1}^{nPTI} P_{PTI(i)}-\sum_{i=1}^{neff} P_{AEeff(i)}\right)*C_{FAE}*SFC_{AE}\right)-\left(\sum_{i=1}^{neff} f_{eff(i)}*P_{eff(i)}*C_{FME}*SFC_{ME}\right)\right]}{f_i*f_c*Capacity*V_{ref}*f_w} \quad (5)$$

$$=\frac{\text{kw}*\frac{\text{g}_{\text{fuel}}}{\text{kwh}}*\frac{\text{g}_{\text{CO2}}}{\text{g}_{\text{fuel}}}}{\text{Tonne*knotical mile / h}}=\frac{\text{g}_{\text{CO2}}}{\text{Tonne*knotical mile}}$$

	Main engine emissions		Aux engine emission		Transport work		Energy saving technology(main power)
	Shaft generators/ Motors emissions and energy saving technologies(Auxilliary power)						

2.1.3 Application And Method Of Calculation

The attained EEDI shall be calculated for ships which falls into one or more of the categories of the vessels mentioned in table 2 of 400GRT and above for,

- A ship for which the building contract is placed on 1January 2013 or,
- In the absence of a building contract the keel laid on or after 1 July 2013.
- The delivery of which is on or after 1 July 2015.
- Substantially alters the dimension, carrying capacity or engine power or major repair.

EEDI value of new ships is required to be less than the baselines representing existing ships by a certain factor. Attained EEDI ≤ [(1-X/100) x Reference line value] where X, the reduction factor as in table 1 and reference value in table 2. Values for bulk carrier is found in table 1 and similar factors for others vessels are found in the IMO Resolution MEPC 203 (62).

Table 1: EEDI reduction factor in % relative to Reference line, MEPC 203 (62) for a bulk carrier**.

Ship type	Size	Phase 1 1Jan'15-31 Dec'19	Phase 2 1Jan'20-31 Dec'24	Phase 3 1Jan'25 onwards
Bulk carrier	≥20000 DWT	10	20	30
	10000-20000 DWT	$0-10^{*}$	$0-20^{*}$	$0-30^{*}$

** Phase 0 elapsed and not shown.

*Reduction factor to be linearly interpolated between the two values dependent upon vessel size. The lower value of the reduction factor is to be applied to the smaller ship size.

Table 2: Reference line value = axb^{-c}, values of *a, b and c,* MEPC 203 (62):

Ship type	A	B	C
Bulk carrier	961.79	DWT	0.477
Gas tanker	1120.0	DWT	0.456
Tanker	1218.8	DWT	0.488
Container ship	174.22	DWT	0.201
General cargo ship	107.48	DWT	0.216
Refrigerated cargo carrier	227.01	DWT	0.244
Combination carrier	1219.0	DWT	0.488
Ro-Ro cargo ships	1405.15	DWT	0.498
Ro-Ro Passenger ships	752.16	DWT	0.381
LNG carriers	2253.7	DWT	0.474
Vehicle / car carriers	(DWT/GT)- 0.7x780.36 where DWT/GT)< 0.3 1812.63 where DWT/GT)≥ 0.3	DWT	0.471
Cruise passenger having non conventional propulsion	170.84	GT	0.214

2.1.4 Reduction Factors And Implementation

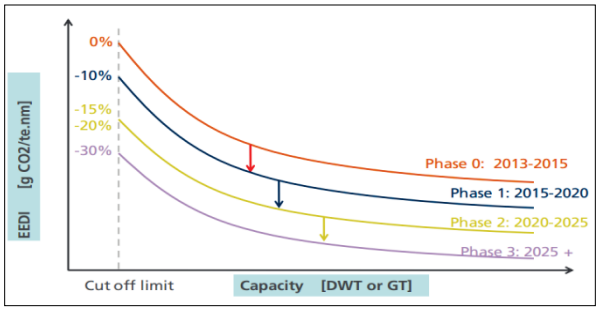

Figure 7: Reduction in phases [15]

At the beginning of phase 1 and at the midpoint of phase 2, IMO will review the status of technological development and if required amendments can be made to the time periods, the EEDI reference line parameters for relevant ship types and reduction rates set out in this regulation. Reduction factors will be used to implement the EEDI in phases so as to gradually reduce the required EEDI in much the same way as NOx and SOx limits.

2.1.5 Significance Of EEDI Regulation

According to IMO the adoption of mandatory reduction measures for all ships from 2013 and onwards will lead to significant emission reductions and cost savings (figure 3). It is predicted that by 2020 annual CO_2 reductions would lie between 100 and 200 million tonnes due to the introduction of EEDI for new ships and the SEEMP for all ships in operation and by 2030 reductions will increase to between 230-420 million tonnes annually which is approximately 10-17% below business as usual by 2020 and between 19-26% in 2030.

3 PROPELLER RELOCATION A SOLUTION FOR EEDI

Figure 8: Propeller concept [18]

Increasing the propeller diameter together with low rotational speed reduces axial and rotational losses there by propulsive efficiency can be improved. But the constraints in the form of hull and ship baseline restrict this. Much research have been done so far by increasing the propeller diameter in the original position and in this work the large area propeller is moved axially aftwards to two positions between the initial location and transom where there was ample space to install it, as demonstrated in an R&D project Streamline [7] initiated by the seventh frame work of European commission. The same concept is tested in this work to study its applicability for optimum EEDI values.

3.1 Modeling Fluid Flow

The equations of fluid flow is a representation of three distinct non linear PDEs. Many assumptions and simplifications has to be made to obtain an incompressible fluid. Even in their reduced form the incompressible fluids case is still non-trivial to solve. Along with the continuity equation the three equations create a complete mathematical system of governing in compressible flow. Reynolds stress tensor arising out of averaging of turbulence will result in more unknowns resulting a closure problem. Numerical methods are employed and the effects of the turbulence can be modeled since we are only interested in the mean. The simplest model is to introduce a turbulent viscosity as a proportionality constant between the Reynold's stress components and the strain rate tensor, in analogy with Newtonian fluids. Introducing this in to the Reynolds average equations gives,

$$\frac{\delta U_i}{\delta t} + U_j \frac{\delta U_i}{\delta x_j} = \frac{\delta}{\delta x_j}\left[-\left(\frac{P}{\rho} + \frac{2}{3}k\right)\delta_{ij} + (v + v_T)\overline{E_{ij}}\right] = -\frac{1}{\rho}\frac{\delta P}{\delta x_i} + (v + v_T)\nabla^2 U_i \quad (6)$$

where $\overline{E_{ij}}$ is the deformation tensor calculated based on the mean flow. The turbulent viscosity v_T must be modeled and most numerical codes which solves the Navier-Stokes equations for practical applications uses some kind of model for v_T.

3.1.1 Various solution methods in Star-CCM+

Finite volume method utilizes the integral form of the conservation laws (Navier-Stokes equations) by separating a computational domain into a series of finite arbitrary control volumes without change of the coordinate system. The method used in Star-CCM+ is of second order accurate in space depending on the convection differencing scheme used. Discretised form of the Navier-Stokes equation shows linear dependence of velocity on pressure and vice versa. This inter equation called velocity pressure coupling is solved by SIMPLE algorithm in this software. It also uses a two-phase Volume of Fluid (VOF) method to calculate the location of the water surface (resolve the boundary between two phases of liquid) as proposed by (Hirt and Nicholas 1981).

4 SIMULATIONS

Numerical self propulsion tests for various propeller locations were performed in a model scale in CFD software Star-CCM+ (Version 9.04.009), with 16GB DDR3- 1600 RAM, Intel® Core i5-4570 CPU @3.2 GHZ (4 core) configuration.

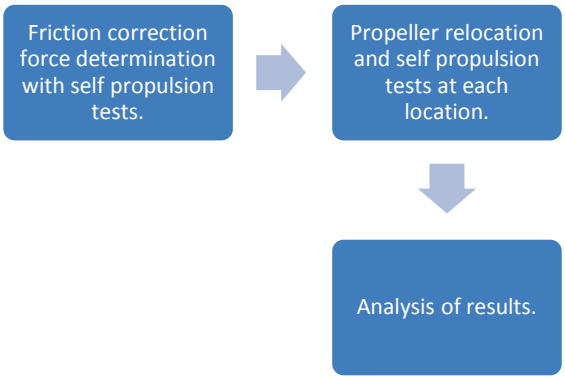

Figure 9: Work flow

The tests were carried out in a research vessel M/S Nawigator belonging to University of Szczecin and the propeller was an indigenous design of Ship Design and Research Centre (CTO S.A). The 3D-CAD file was developed in NAPA IGES format.

4.1 PROPELLER SPECIFICATION

Table 3: Open water characteristics of propeller used.

Propeller1 specification	
No blades/ Rake/ Skew	4/0/20˚
NACA profile mean line	16/0.8
Diameter (mm)	226
Pitch ratio at 0.7R (P/D)	0.942
Exp area ratio	0.673
Hub ratio	0.3
Blade width at 0.7R (mm)	102.4
Propeller RPS (anticlockwise)	19

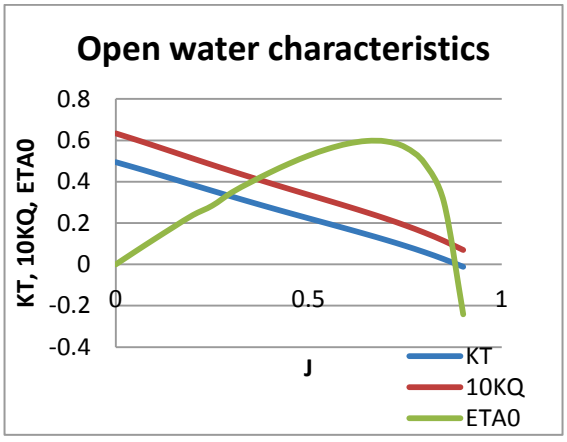

Figure 10: Propeller open water diagram

4.1.1 The Computational Model

The grid in the propeller region rotates around the stationary propeller. The grid in the tank remains stationary (not rotating). The two grids slide past each other at a cylindrical interface. In the tank region the standard conservation equations for mass and momentum are solved. In the sliding mesh model motions of the propeller region is accounted by a grid motion of the propeller domain and the flow variables are interpolated across the sliding interface. In this unsteady problem all interaction effects can be determined accurately. The computations were carried out for a model speed corresponding to Fn= 0.22 and $RN_M = 8.37x10^6$

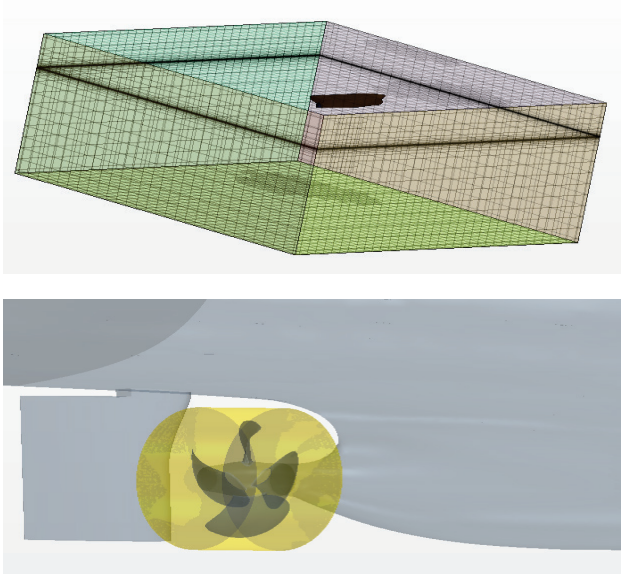

Figure 11: Fig (Top): Computational domain, Fig (Bottom): Sliding interface around propeller.

4.1.2 Mesh Considerations

Trimmed mesh is utilized in the computational domain. This type of mesh provides a robust and efficient method of producing a high quality grid for both simple and complex mesh generation problems and is very efficient to refine the cells in a wake region. Polyhedral mesh is used in the rotating domain around propeller as they provide a balanced solution for complex mesh generation problems. They are relatively easy and efficient to build requiring no more surface preparation than the equivalent tetrahedral mesh. As shown in figure 12 local refinements were done near free surface and in the aft region of the ship where flow separation and viscous effects are predominant. 1.2million cells were used for this calculation.

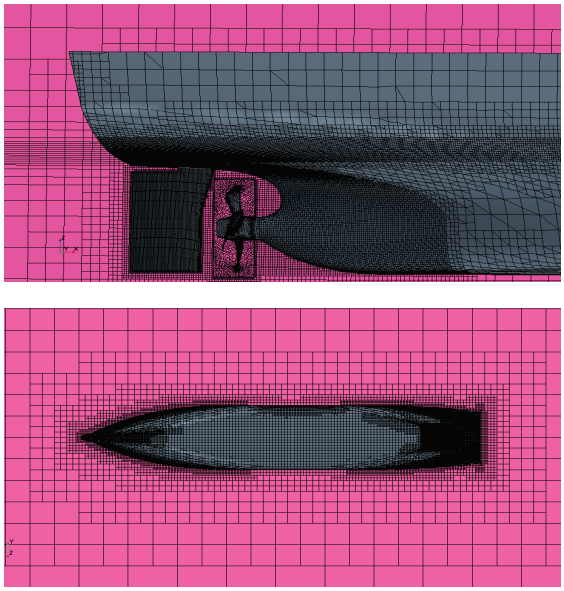

Figure 12: Mesh refinement in various zones.

4.1.3 Physical Model

Computations of flow around the ship hull with rotating propeller simulating propulsion tests have an unsteady character and therefore need more time to obtain convergence. So implicit unsteady model with Realizable K-Epsilon two layer turbulence model has been chosen and Volume of Fluid (VOF) method is utilized [6].

4.1.4 Setting Solver Parameters

The simulation is transient for which the appropriate time step, the number of inner iterations per time step are important. The required time step of 200 time steps per period is required. But according to the simulations performed earlier at CTO S.A, a 10 times larger time step is sufficient to compare the models and the same is applied. Appropriate under relaxation factors were introduced to enhance convergence.

4.1.5 External Towing Force

The friction correction force (SFC) is evaluated by selecting a force monitor including the propeller blade, boss, rudder and hull. The resultant force gives the additional friction correction force that is applied to the model.

4.1.6 Convergence Analysis

The results in figure 13 shows that a physical time of 30 seconds (24 hours in actual) can be considered for getting an appropriate convergence and for the simulations this time interval was chosen as a stopping criteria since the objective is to compare the models.

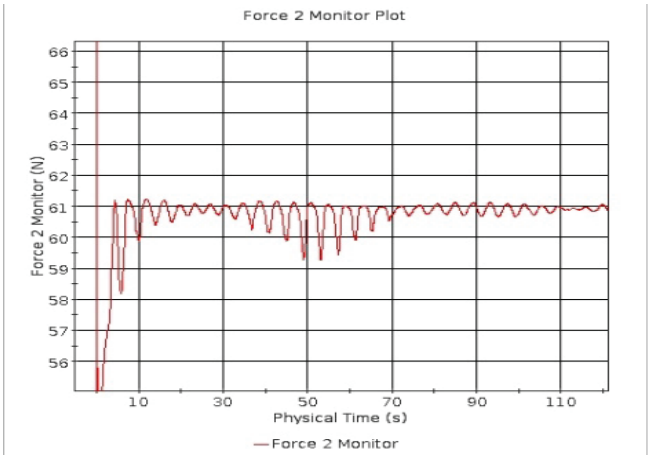

Figure 13: Thrust monitor plot

4.2 VALIDATION OF NUMERICAL ANALYSIS

The results in table 4 shows a considerable difference of friction correction force (SFC), thrust and torque because of higher chosen time step. Nevertheless it is valid because the aim was to compare the self propulsion results of various cases.

Table 4: EFD vs CFD results

	Experiments	STAR-CCM+	Error %*
Diameter(m)	0.226		
Speed(m/sec)	1.609		
Rps	8.99		
SFC (N)	3.81	3.50	8
Thrust (N)	50.67	42.00	16.12
Torque (N.m)	1.70	1.53	8.02
Resistance (N)	-	41.5	
Delivered power (Watts)	95.78	86.40	

*Error percentage calculated as $\left(\frac{Ref-Com}{Ref}\right) x\ 100$ where Ref is the experimental data taken as reference and Com is the value compared which is the Star-CCM+ results.

4.3 PROPELLER RELOCATION

Figure 14: Propeller moved aft

In case1 the rudder is removed from the ship for the experiments and the propeller is relocated axially aft to two different positions just before the stern similar to Knutsson et.al.,2011. At each position self propulsion tests were carried out with three sets of RPM and based on this, the results were interpolated for the skin friction correction (SFC) as obtained in the numerical self propulsion initially done with rudder. **Propeller1 (table 3)** is used in this simulation. It is mentioned as **OP** in the graphs. In case 2 the propeller diameter was enlarged by 15% **(propeller 2)** keeping other ratios constant and tests repeated.

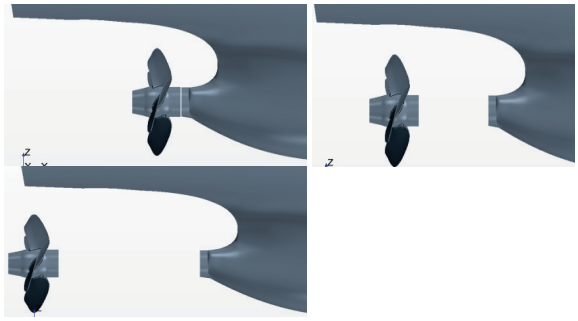

Figure 15: (Clockwise from top) Position 0, 1, 2 resp.

Table 5: Case1 results based on thrust identity.

	Pos0	Pos1	Pos2
Rps	9.51	9.496	9.535
SFC (N)	3.81	3.81	3.81
K_T	0.26	0.222	0.207
K_Q	0.038	0.0348	0.0334
Thrust deduction (t)	0.38	0.280	0.231
K_{QOM}	0.038	0.0335	0.032
J	0.75	0.75	0.75
J_{TM}	0.465	0.51	0.53
W_{TM}	0.381	0.32	0.29
Open water efficiency (η_{OTM})	0.51	0.54	0.545
Hull efficiency (η_{HM})	0.998	1.058	1.084
Rotative efficiency (η_{RT})	0.99	0.961	0.958
Propulsive efficiency (η_D)	0.504	0.549	0.566

5 ANALYSIS OF RESULTS

Table 6: Comparison (in %) with reference to the initial propeller location of case1

	Propeller1			Propeller2		
	Pos0	Pos1	Pos2	Pos0	Pos1	Pos2
η_{OTM} *	Ref*	6.15	7.16	2.7	14.5	13.3
η_{HM}	Ref	5.97	8.55	-7.3	-4.89	-0.89
η_{RT}	Ref	-3.17	-3.43	-0.45	-4.13	-4.6
η_D	Ref	8.92	12.34	-5.18	4.41	7.07
Del power	Ref	-8.19	-10.98	5.5	-4.22	-6.59

*Ref- Reference, Pos- Position.

*Variation calculated as $-\left(\frac{Ref-Com}{Ref}\right) x\ 100$ where Ref is the reference value and Com is the value compared.

5.1.1 Thrust Deduction And Wake Fraction

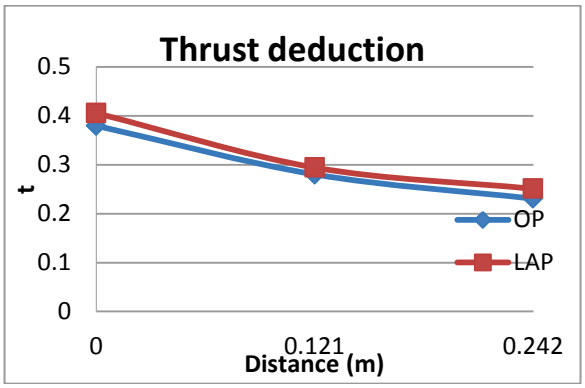

Figure 16: Position vs Thrust deduction

As shown in figure 16 the thrust deduction factor (t) drops rapidly when moving the propeller aft from its original position. The wake fraction (figure 17) also shows the same behavior.

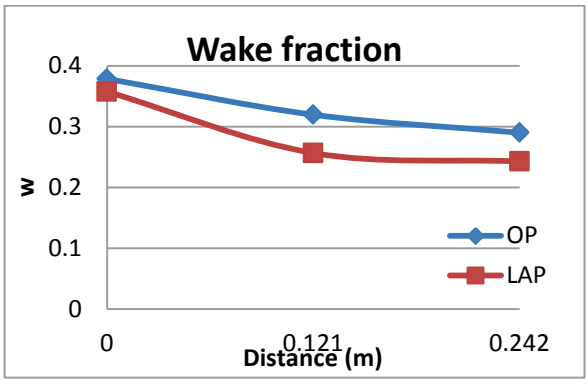

Figure 17: Position vs Wake fraction

5.1.2 Hull Efficiency And Total Resistance

Hull efficiency is higher with both the propellers for the whole range (figure 18). To illustrate the physics behind development of hull efficiency, the pressure distribution on the aft part of the hull is also shown in figure 20 and the axial velocity at a cut just infront of the propeller plane is shown for two positions in figure 21 for propeller1 (propeller2 behavior was similar).

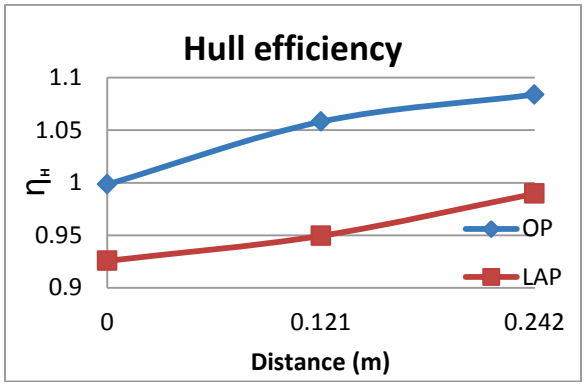

Figure 18: Position vs Hull efficiency

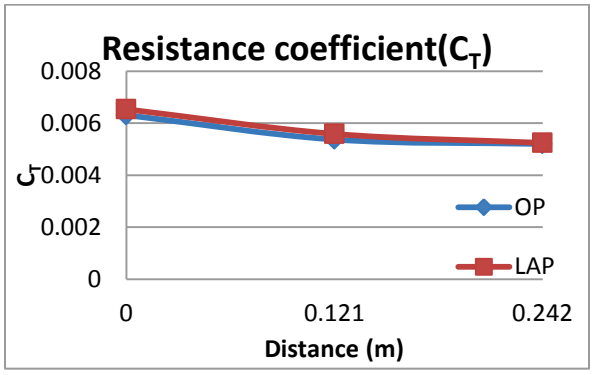

Figure 19: Position vs resistance coefficient

As shown in figure 20 the pressure on the hull increases when moving the propeller aft. When a propeller operates closer to the hull it increases the flow velocity in front of the propeller disc and thereby reduces the pressure on the hull. This is the main cause of thrust deduction and as a result of this there is also an increased friction.

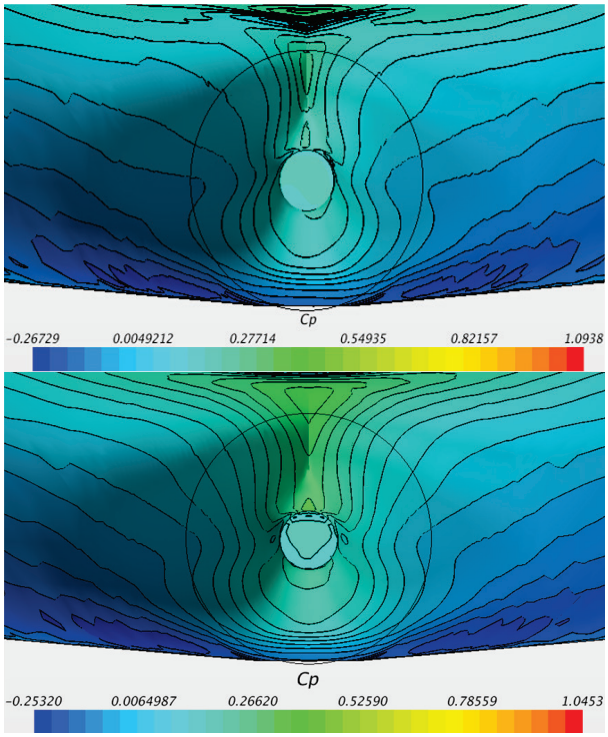

Figure 20: Pressure on the hull: Position 0 (Top) Position 2 (Bottom).

When propeller operates away from the hull the flow velocity increases and it operates closer to the free stream velocity when moving the propeller aft.

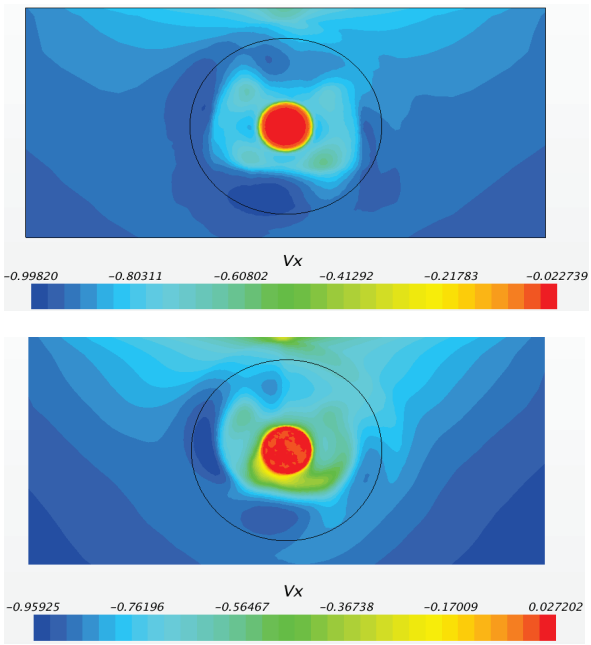

Figure 21: Velocity profile just upstream of the propeller plane: Pos 2 (Top), Pos 0 (Botttom).

Water inflow velocity is measured with a line probe just upstream of the propeller in the transverse axis at a distance corresponding to the centre of propeller from the keel (velocity opposite to ships motion hence -). Figure 22 shows an increase of velocity with position 2 for the chosen propeller. Similar trend was observed for both the propellers [negative sign (-) implies velocity downstream of propeller according to the chosen axis].

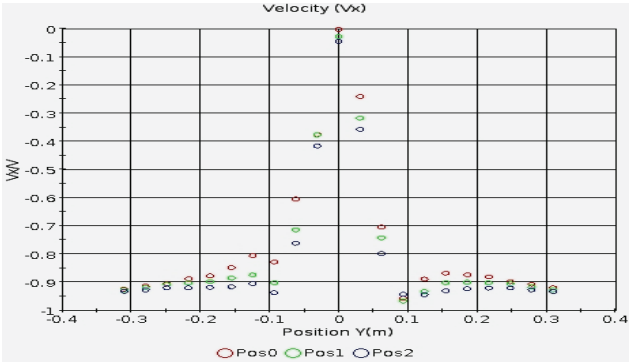

Figure 22: Velocity just upstream of the propeller in a line along *y* axis.

5.1.3 Rotative And Open Water Efficiency

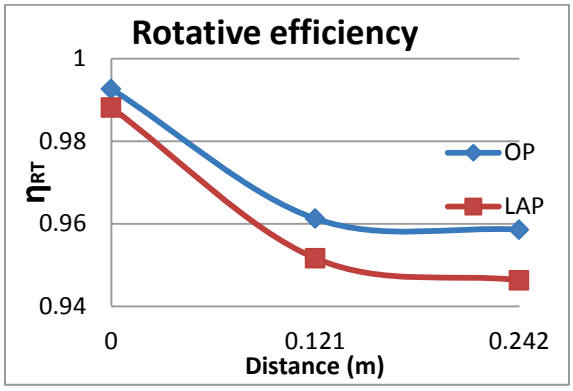

Figure 23: Position vs Rotative efficiency

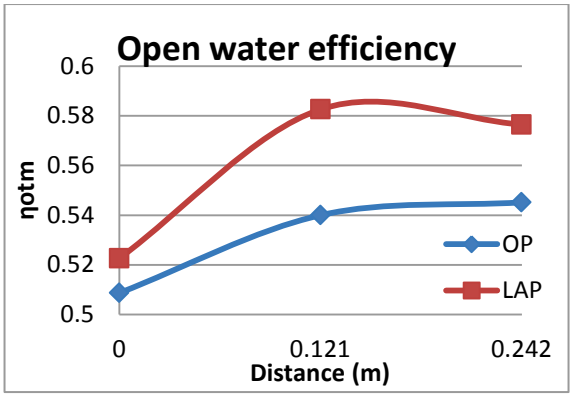

Figure 24: Position vs open water efficiency

Figure23 shows, for the original position the rotative efficiency is higher for both the propellers where the wake is non homogeneous. It decreases with distance from the hull. In the uneven wake flow the drag of the propeller sections is reduced due to Katzmayr [8] effect which results in a reduction of K_Q for a given K_T. Another reason is that the propeller is wake adapted i.e., designed for the hull wake. They may thus be less efficient in a homogeneous inflow. The propeller open water efficiency is shown in figure 24 for both propellers and positions. Propeller2 shows a significantly higher larger efficiency and this really shows the main reason for choosing the large area propellers for ships. It has to be noted that both propellers operate close to optimum working point.

5.1.4 Propulsive Efficiency And Delivered Power

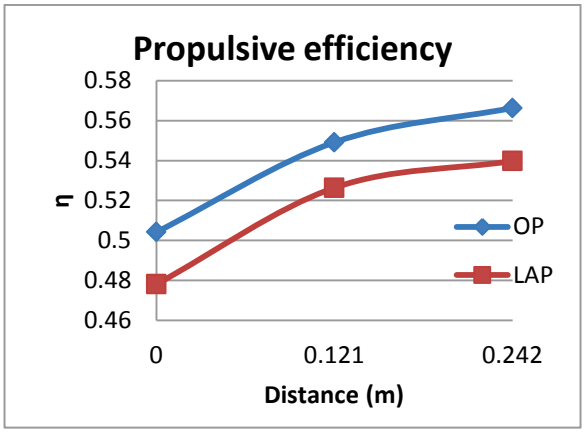

Figure 25: Position vs Propulsive efficiency

Having analyzed all contributions to the final efficiency the figure 25 shows the variation of the total efficiency. The reason for the increase of efficiency is the open water and hull efficiency which increases more than the decrease in relative rotative efficiency.

The extraction [8] of energy from unsteady flows using a stationary foil is called the Katzmayr effect, after the German engineer who first studied it in 1922. He did experiments in the wind tunnel by mounting an airfoil in the open test section while subjecting the air stream to periodic oscillations.

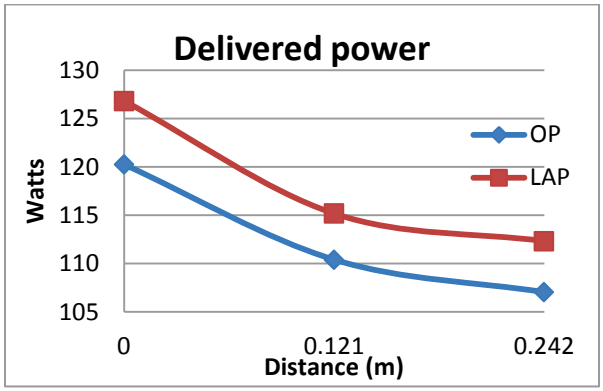

Figure 26: Position vs Delivered power (R)

The minimum delivered power is obtained for Position2 for both the propellers (figure 26). Also a very interesting trend is noticed here even when the propeller is moved a few distance away from its original position there is 8% decrease of delivered power for the original propeller.

Table 7: Delivered power comparison with positions.

	Propeller1			Propeller2		
	Pos0*	Pos1	Pos2*	Pos0	Pos1	Pos2
Del power	Ref	-8.19	-10.98	5.5	-4.22	-6.59

*Pos 0- Position 1, Pos2- Position 2.

5.1.5 Velocity Vector

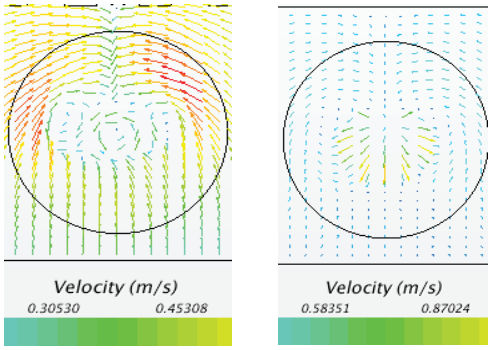

Figure 27: Velocity vector just upstream of propeller plane. Position 0 (L) Position 2 (R).

A plane just upstream of the propeller plane is chosen to study the vortices which is an important parameter for vibrations and observed to be reduced when moving the propeller aft as seen in figure 27.

6 APPLICATION OF EXPERIMENTAL RESULTS

The analyzed vessel is a research vessel and it is not included in the EEDI formulation by IMO. Nevertheless the percentage of (value obtained for propeller1 at position1 is chosen for analysis) delivered power reduction attained in model scale (full scale prediction yielded unrealistic results which needs further investigation) is analyzed against its influence on the EEDI factor of a bulk carrier (vessel chosen from a publication of IACS [14]) and the results are summarized in table 8 based on following calculations:

Bulk carrier, MCR Main engine: 6900 kW, DWT- 55000 Tons, Service speed: 14.25 Knots.

Attained EEDI

$$= \frac{(6900x3.206x171)+(381x3.206x205)}{(1.017x\ 55000x\ 14.25)} = \mathbf{5.06\ g/\ t.nm}$$

(It is not a straight forward comparison, it is demonstrated to show the influence of power savings in percentage with respect to the EEDI vale):

Table 8: Validity of relocation concept

Attained EEDI	Requirement (Phase 0)	Requirement (Phase 1)	Result
5.06 g/t.nm	5.27 g/t.nm	4.74 g/t.nm (10% margin reduced)	Valid in phase 0 but for phase1
Delivered power gain of 8.2% resulted in 4.66 g/t.nm			Phase 1 requirement satisfied

7 CONCLUSION

Moving the propeller aft indicated some interesting trends in the propulsion factors. Even though the delivered power of the large area propeller can't be reduced more than the default propeller, the trends have been analyzed, and based on this an optimum propeller with appropriate Pitch/ Diameter (P/D) ratio can be chosen in future.

When the propeller moved aft, there is a very good trend of decrease in delivered power. The reason for the increase of efficiency in these experiments are, the open water and hull efficiency which increased more than the decrease in relative rotative efficiency. While moving the propeller aft the clearance also increased for the propellers considered. This can result in a reduction of pressure pulses, which is most crucial for vibration and fatigue problems.

This investigation was carried out without rudder and optimization methods. Hence if those are considered, greater power reduction will be achieved.

It can be concluded that if a large area propeller is fixed in an appropriate location behind the ship significant amount of power savings can be realized, which is the key factor to satisfy the more stringent EEDI phases in future.

8 FUTURE WORK

The work can be continued by choosing an optimum P/D ratio as demonstrated in the experiments done by the leading propulsion engine manufacturer MAN-B&W [17], and in a research work done at Chalmers University by Knutsson et al., with large area propellers, both resulted in considerable increase of propulsion efficiency.

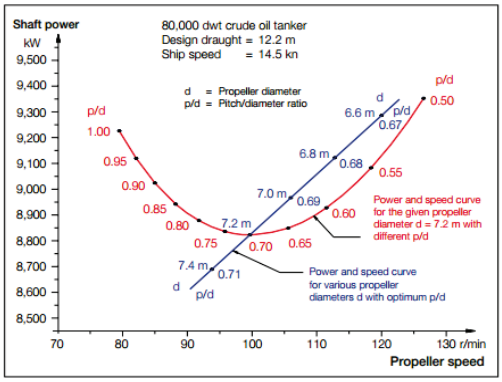

Figure 28: Influence of P/D ratio in propeller design [17]

9 ACKNOWLEDGEMENTS

This work was developed in partial fulfillment of the requirements for the double degree program "Advanced Master in Naval Architecture" conferred by University of Liege, "Master of Sciences in Applied Mechanics, specialization in Hydrodynamics, Energetics and Propulsion" conferred by Ecole Centrale de Nantes. Master thesis developed at West Pomeranian University of Technology, Szczecin (www.emship.eu).

I would like to thank my professors in the EMSHIP study program and *Ship Design and Research Centre (CTO S.A.),* for giving me an opportunity to pursue this work. This thesis was developed in the frame of the European Master Course in “Integrated Advanced Ship Design” named “EMSHIP” for “European Education in Advanced Ship Design”, Ref.: 159652-1-2009-1-BE-ERA MUNDUS-EMMC.

10 REFERENCES

[1]*Third IMO GHG Study 2014*, International Maritime Organization (IMO), July 2014

[2] *Second IMO GHG Study 2009*, International Maritime Organization (IMO) London, UK, April 2009; Buhaug, Ø., Corbett, J.J., Endresen, Ø., Eyring, V., Faber, J., Hanayama, S., Lee, D.S., Lee, D., Lindstad, H.,Markowska, A.Z., Mjelde, A., Nelissen, D., Nilsen, J., Pålsson, C., Winebrake, J.J., Wu, W., Yoshida, K.

[3] IPCC, 2007: Climate Change 2007: Synthesis Report. Contribution of Working Groups I, II and III to the Fourth AssessmentReport of the Intergovernmental Panel on Climate Change [Core Writing Team, Pachauri, R.K and Reisinger, A.(eds.)]. IPCC, Geneva, Switzerland, 104 pp.

[4] United States Environmental Protection Agency (EPA) report. http://www.epa.gov/climatechange/ghgemissions/gases/co2.html

[5] Heitmann, Nadine, and Setareh Khalilian. "Accounting for carbon dioxide emissions from international shipping: Burden sharing under different UNFCCC allocation options and regime scenarios." *Marine Policy* 35.5 (2011): 682-691.

[6] Bugalski, Tomasz, and Paweł Hoffmann. "Numerical Simulation of the Self-Propulsion Model Tests." *Proceeding of 2nd International Symposium on Marine Propulsors*. 2011.

[7] Knutsson, Daniel, and Lars Larsson. "Large area propellers." *SMP'11 (Symposium on Marine Propulsors*. 2011.

[8] Katzmayr, R., Effect of periodic changes of angle of attack on behavior of airfoils, NACA TM 147, October 1922.

[9] Resolution mepc.212(63), annex 8, resolution mepc.212(63), adopted on 2 march 2012, 2012 guidelines on the method of calculation of the attained energy efficiency design index (EEDI) for new ships.

[10] MEPC 63/23, Annex9, resolution mepc.213(63),adopted on 2 march 2012, 2012 guidelines for the development of a ship energy efficiency management plan (SEEMP).

[11] IMO Guidelines for voluntary use of the Ship Energy Efficiency Operational Indicator (EEOI), MEPC.1/Circ.684, 17 August 2009

[12] Kanu Priya Jain, "Impacts of Energy Efficiency Design Index", Newcastle University, (2012).

[13] S.M. Rashidul Hasan, "Impact of EEDI on Ship Design and Hydrodynamics" Department of Shipping and Marine Technology, Chalmers University of Technology (2011).

[14] Procedure for calculation and verification of theEnergy Efficiency Design Index (EEDI), International Association Of Classification Societies Ltd IACS Proc Req. 2013.

[15] Implementing EEDI, a guidance for owners, operators, shipyards and tank testing organisations, Lloyd's Register (2012).

[16] Historic background of emission regulations, IMO. http://www.imo.org/OurWork/Environment/PollutionPrevention/AirPollution/Pages/Historic%20Background%20GHG.aspx

[17] Basic Principles of Ship Propulsion, MAN Diesel & Turbo. http://marine.man.eu/docs/librariesprovider6/propeller-aftship/basic-principles-of-propulsion.pdf?sfvrsn=0

[18] www.joules-project.eu

[19] Prabu Duplex, “Novel application of large area propeller to optimize Energy Efficiency Design Index (EEDI) of ships”, Master thesis, Emship.

11 AUTHORS BIOGRAPHY

Prabu Duplex is pursuing a Professional Doctorate in Engineering (PDEng) program at the University of Twente in The Netherlands. He is presently developing physics based mathematical models, to predict the life time of diesel engine components, in maritime propulsion system. He had completed his masters degree in naval architecture in the year 2015, in which he specialized in hydrodynamics, computational fluid dynamics, ship structural engineering and production technology.

Marek Kraskowski, is the Deputy Head of Hydro mechanics division, **Tomasz Bugalski**, is a senior

specialist and **Pawel Hoffman** is a computational fluid dynamics specialist. They are presently working in hydromechanics division of Ship Design and Research Centre in Poland. Ship Design and Research Centre is a specialist R&D, design and general technology unit, operating for the maritime industry in particular.

Zbigniew Sekulski is working as an assistant professor, at West Pomeranian University of Technology (ZUT) in Poland. His research domain includes ship structural engineering and multi objective optimization.